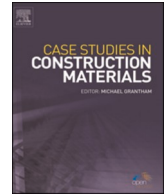




ELSEVIER

Contents lists available at ScienceDirect

Case Studies in Construction Materials

journal homepage: www.elsevier.com/locate/cscm

Case study

Self-compacting steel fibers reinforced geopolymer: Study on mechanical properties and durability against acid and chloride attacks

Piti Sukontasukkul^{a,*}, Darrakorn Intarabut^a, Tanakorn Phoo-ngernkham^b, Cherdsak Suksiripattanapong^c, Hexin Zhang^d, Prinya Chindapasirt^{e,f}^a Construction and Building Materials Research Center, Department of Civil Engineering, King Mongkut's University of Technology, North Bangkok, Bangkok 10800, Thailand^b Sustainable Construction Material Technology Research Unit, Department of Civil Engineering, Faculty of Engineering and Technology, Rajamangala University of Technology Isan, Nakhon Ratchasima 30000, Thailand^c Department of Civil Engineering, Faculty of Engineering and Technology, Rajamangala University of Technology Isan, Nakhon Ratchasima 30000, Thailand^d School of Computing, Engineering and the Built Environment, Edinburgh Napier University, Scotland EH10 5DT, UK^e Sustainable Infrastructure Research and Development Center, Department of Civil Engineering, Faculty of Engineering, Khon Kaen University, 40002, Thailand^f Academy of Science, Royal Society of Thailand, Dusit, Bangkok 10300, Thailand

ARTICLE INFO

Keywords:

Self-compacting geopolymer
 Self-compacting Fiber reinforced geopolymer
 Flow and fill ability
 Durability
 Chloride migration
 Acid attack

ABSTRACT

This study aimed to investigate the effects of steel fibers on the properties of self-compacting geopolymer (SCG), including flowability and fillability, compressive and flexural strength, and durability against harmful chemical substances such as acids and chloride. In the first stage, the study involved determining the optimum fiber content for geopolymer that meets the criteria for self-compacting concrete. The second stage involved investigating the mechanical properties and durability of self-compacting fiber-reinforced geopolymer (SCFRG). For SCG, the binder phase consisted of fly ash and slag at different proportions, while for SCFRG, the geopolymer was mixed with hooked-end steel fiber at 0.5–1.5% by volume fractions. The study found that adding 0.5% to 1.5% steel fibers by volume fraction to create self-compacting fiber-reinforced geopolymer (SCFRG) improved compressive strength by 8.7%, toughness by 88%, and residual strength by 83.7%. However, it slightly reduced slump and filling ratio while increasing T50. Both SCG and SCFRG's durability were assessed by immersing samples in 5% concentration chemical solutions, resulting in weight loss to varying degrees depending on the type of chemical. In terms of weight loss, immersion in 5% sodium chloride showed no effect, while immersion in 5% magnesium sulfate and 5% sulfuric acid resulted in a reduction in weight compared to samples cured in ambient conditions. Additionally, SCFRG samples submerged in MgSO₄, H₂SO₄, and NaCl demonstrated relatively stable compressive strength when compared to ambient samples. The addition of steel fibers to SCG reduced the chloride penetration depth and diffusivity, indicating better resistance to chloride ion penetration. In summary, the study demonstrated that although the addition of steel fibers decreased flowability and fillability, it potentially improved the mechanical and durability properties of self-compacting geopolymer.

* Corresponding author.

E-mail addresses: piti.s@eng.kmutnb.ac.th, piti.kmutnb@gmail.com, piti@kmutnb.ac.th (P. Sukontasukkul).<https://doi.org/10.1016/j.cscm.2023.e02298>

Received 8 May 2023; Received in revised form 3 July 2023; Accepted 8 July 2023

Available online 10 July 2023

2214-5095/© 2023 The Author(s). Published by Elsevier Ltd. This is an open access article under the CC BY license (<http://creativecommons.org/licenses/by/4.0/>).

1. Introduction

Concrete production using Portland cement and raw materials has various environmental impacts, including CO₂ emissions, depletion of natural resources, and consumption of fossil fuels. To address these issues, sustainable cementitious materials are being developed, which aim to reduce Portland cement content or replace it entirely. One common approach is the use of supplementary materials such as fly ash, slag, and silica fume, which significantly decrease the use of Portland cement. Another approach is to find alternative cementitious materials to replace Portland cement partially or entirely in the concrete mixture, and geopolymer is emerging as one of the most promising options.

Geopolymers can be made from various types of alumino-silicate materials, including coal ash, silica fume, calcined clay, and other waste or byproducts containing silica and/or alumina [1]. Compared to conventional Portland cement, geopolymer has a lower carbon footprint and is more environmentally friendly. Geopolymerization involves activating silica and alumina source materials with an alkaline solution, resulting in hardened cement-like products [2]. The structure of geopolymers is composed of silica and alumina tetrahedral coordination with oxygen, and it forms three basic units: polysialate, polysialate-siloxo, and polysialate-disiloxo [3].

Geopolymers possess many desirable properties, including high early strength [4], resistance to sulphate [5], seawater [6], and acidic environments [7], steel corrosion protection [8,9], fire resistance [10–12], and good bonding with steel reinforcement [13–16]. These properties make geopolymer an attractive alternative to conventional Portland cement, and research in this area is ongoing.

Class C fly ash, a type of high calcium fly ash, is a byproduct of coal combustion and is produced in large quantities in countries where coal is used to generate electricity. In Thailand, the Mae-Moh power plant generates a significant amount of class C fly ash annually, which is used as a cement replacement material in concrete production. Geopolymer, which is a promising alternative to Portland cement, commonly utilizes class C fly ash due to its high content of alumina and silica. The use of class C fly ash in geopolymer concrete has several advantages in terms of fresh properties, such as promoting early strength development and enabling room temperature curing. However, it also has some drawbacks, such as fast setting and poor workability [17]. In terms of hardened properties, geopolymer concrete exhibits similar properties to plain concrete, which is strong in compressive strength but weak in tensile strength. To enhance toughness and mechanical properties, short fibers can be added to geopolymer mixes, with the degree of improvement depending on the fiber type and content. Various studies have investigated the effects of fiber addition on geopolymer concrete, and the results indicate that it is an effective approach to improving its mechanical properties [18–24].

In practical construction, the compaction of traditional concrete or geopolymer often requires the use of a vibrator. However, when heavy steel reinforcements are present in structures, achieving proper concrete compaction can be challenging and may necessitate extensive vibrator usage, leading to segregation. The solution to this problem lies in the development of self-compacting concrete (SCC) and self-compacting geopolymer (SCG). These materials can flow effortlessly and fill every corner of the formwork without requiring any compaction. The benefits of using SCC and SCG include easy filling of narrow and restricted sections, good compaction, strong bond strength, quick construction, reduced construction costs, and time savings.

Although various researchers have investigated the development of SCG based on different parameters, such as sodium hydroxide concentration [25,26], sodium silicate/sodium hydroxide ratio [27], superplasticizer [26,28], and silica fume/fly ash/rice husk ash content [29–34], very few of them have examined the effect of fiber on SCG. Given that fibers are increasingly being used to improve the mechanical properties of geopolymer [35–44], it is crucial to investigate their effect on SCG. Therefore, our first objective is to investigate the properties of self-compacting steel fiber reinforced geopolymer based on the requirement specified by EFNARC [44] regarding flow and filling ability of self-compacting concrete.

In addition to investigating properties related to self-compacting concrete, this study aims to assess the durability of SCG and SCFRG against harmful chemical substances such as sulfuric acid, magnesium sulfate, and sodium chloride. Geopolymers have been found to possess excellent resistance to chemical attacks from a range of acids, bases, and salts, including sulfuric acid, magnesium sulfate, and sodium chloride. The high density of the geopolymer matrix and the chemical stability of the aluminosilicate bonds that make up the geopolymer structure are responsible for the resistance of geopolymers to chemical attack. While there are numerous studies exploring the durability of geopolymer and fiber reinforced geopolymer against harmful chemical substances [46–53], very few of them have been conducted in the field of self-compacting steel fiber reinforced geopolymer [54,55]. However, still they are not adequate to fill the gap in this area so further study is required.

This study investigated the effect of steel fiber addition on the properties and durability of self-compacting geopolymer (SCG), using Class-C fly ash and slag as base raw materials. Hooked end steel fibers were incorporated into SCG at rates of 0.5–1.5% by volume to produce self-compacting SCFRG, and experiments were conducted according to EFNARC guidelines to assess both fill- and flow-abilities. The study also examined the impact of fibers on the compressive strength and flexural performance of hardened SCFRG, as well as its durability against exposure to chloride, sulfuric acid, and magnesium sulfate. The durability study included assessments of weight loss and mechanical change after exposure to chemical substances for a certain period, and determination of chloride penetration and diffusion using rapid chloride migration test.

2. Experimental procedure

2.1. Materials

The materials utilized in this research comprised of high calcium fly ash (FA) with a specific gravity of 2.61 and chemical composition, which can be found in Table 1. Additionally, ground slag (SL) with a specific gravity of 2.90 and chemical composition

Table 1
Chemical compositions of FA and SL.

Mineral type	Oxide (%)								
	SiO ₂	Al ₂ O ₃	Fe ₂ O ₃	CaO	MgO	K ₂ O	Na ₂ O	SO ₃	LOI
FA	31.9	15.9	14.1	26.8	3.7	2.0	2.0	2.5	0.2
SL	32.3	15.4	0.6	39.0	7.2	0.4	0.7	1.2	0.7

provided in Table 1 were used, along with river sand with a specific gravity of 2.85 and particle size ranging from 1.19 to 4.75 mm. The other materials included sodium hydroxide solution (NaOH) with concentrations of 8 and 12 molar, sodium silicate solution (Na₂SiO₃), hooked-end steel fiber with an aspect ratio of 65 (see Table 3), and superplasticizer type G (ASTM C 494) Table 2.

2.2. Mix proportion

The binder phase was composed of FA and SL in an 80/20 ratio, while the superplasticizer content remained constant at 2.5% of the binder weight. The sand/binder and NaOH/Na₂SiO₃ ratios were set at 1.25 and 1, respectively, and the liquid/binder ratios were 0.40 and 0.45. Three different fiber volume fractions of 0.5%, 1.0%, and 1.5% were used to create self-compacting geopolymer (SCG) and fiber-reinforced geopolymer (SCFRG). Please refer to Table 3 for the detailed mix proportions of SCG and SCFRG.

The mixing process began by dry mixing FA, SL, and sand for 1 min. After that, the NaOH solution was added, and the mixing continued for another 2 min. Next, the sodium silicate solution was added, and the mixing continued for an additional 2 min. Lastly, the fibers were dispersed uniformly throughout the fresh mix, and the mixing continued for 1–2 min until all fibers were fully and uniformly distributed.

After finishing the mixing, the fresh mixes were subjected to a series of flow and fill tests, as described in Section 2.3, and then cast into 100×100×100 mm cubic and 100×100×350 mm prism specimens. All specimens were wrapped with plastic sheet until the date of the test, which was 28 days later.

2.3. Experimental series

The experimental sequence involved the following steps:

- 1) Fresh SCG and SCFRG underwent three tests (flow, T50, and L-box) based on EFNARC guidelines for self-compacting concrete, requiring passing and filling as per Table 4.
- 2) Samples that met the EFNARC requirements were selected for compression and flexural performance tests.
- 3) The mix proportion that passed EFNARC and yielded the highest strengths was selected for durability testing.

Table 2
Properties of hooked end steel fiber.

Properties	Shape	Material	Length (mm)	Diameter (mm)	Tensile strength (N/mm ²)	Aspect ratio
Description	Hooked end	Steel	35	0.55	1345	65

Table 3
Detail mix proportion for plain and fiber reinforced geopolymer.

Designation	Liquid/Binder Ratio	NaOH Con. (M)	Fly ash (g)	Slag (g)	River sand (g)	Steel Fiber (%)	Super (%)
0.4/8/SCG	0.40	8	80	20	125	-	2.5
0.4/8/0.5SCFRG	0.40	8	80	20	125	0.5	2.5
0.4/8/1.0SCFRG	0.40	8	80	20	125	1.0	2.5
0.4/8/1.5SCFRG	0.40	8	80	20	125	1.5	2.5
0.45/8/SCG	0.45	8	80	20	125	-	2.5
0.45/8/0.5SCFRG	0.45	8	80	20	125	0.5	2.5
0.45/8/1.0SCFRG	0.45	8	80	20	125	1.0	2.5
0.45/8/1.5SCFRG	0.45	8	80	20	125	1.5	2.5
0.4/12/SCG	0.40	12	80	20	125	-	2.5
0.4/12/0.5SCFRG	0.40	12	80	20	125	0.5	2.5
0.4/12/1.0SCFRG	0.40	12	80	20	125	1.0	2.5
0.4/12/1.5SCFRG	0.40	12	80	20	125	1.5	2.5
0.45/12/SCG	0.45	12	80	20	125	-	2.5
0.45/12/0.5SCFRG	0.45	12	80	20	125	0.5	2.5
0.45/12/1.0SCFRG	0.45	12	80	20	125	1.0	2.5
0.45/12/1.5SCFRG	0.45	12	80	20	125	1.5	2.5

Note: a/bSCG refers to self-compacting geopolymer and a/b/cSCFRG refers fiber reinforced self-compacting geopolymer, where a = L/B ratio, b = NaOH concentration, and c = fiber volume fraction

The test sequence flow chart is illustrated in Fig. 1.

The ASTM C1611 standard was used to conduct flow and T50 tests, which aim to evaluate the filling ability of fresh geopolymer. Prior to testing, the slump cone and base plate were cleaned and moistened with water. The test procedure involves filling the slump cone with fresh geopolymer without tamping, removing excess material, slowly lifting the cone vertically to allow the geopolymer to flow freely, and recording the time and final diameter after the flow stops. The final diameter is the average of two perpendicular measurements and is called the "slump flow," while the time taken for the geopolymer to flow to the 500 mm mark is referred to as T50.

The L-box test, a standard method for testing fresh self-compacting concrete, was performed according to BS EN 12350–10. The aim of the test is to assess the ability of self-compacting concrete to pass through obstacles. The L-box apparatus comprises a vertical hopper and a horizontal flow tank, with two types of obstacles consisting of two or three rebars with three or four openings. The test procedure involves cleaning and moistening the inside of the L-box, closing the gate, placing the obstacle, and filling the vertical hopper with geopolymer. After one minute, the gate is opened, allowing the geopolymer to flow through the obstacle and into the flow tank. Once the flow stops, the heights of geopolymer at the end of the flow tank (H2) and the height left in the vertical tank (H1) are measured to calculate the passing ratio by dividing H2 by H1. A schematic representation of the L-box apparatus and test procedure is presented in Fig. 2.

The compression test was conducted based on EN 12390–3:2019: Testing hardened concrete - Part 3: Compressive strength of test specimens. Since the test method for compressive strength of hardened concrete is quite well-known, the testing detail is omitted in this manuscript.

The flexural performance test was carried out based on ASTM C1609: Standard Test Method for Flexural Performance of Fiber-Reinforced Concrete (Using Beam with Third-Point Loading) (Fig. 3). The test process begins with placing the specimen on the support, mounting two LVDTs on the moving jig, securing the jig on the specimen, adjusting the LVDT tip to touch the steel plate, and loading the specimen at the rate of 0.025–0.075 mm/minute (0.0015 and 0.004 in/min) until the desired deflection (L/150) is reached. Using the recorded data, the load vs deflection curves are plotted and used in calculating the parameters such as toughness and residual strength at the deflection of L/300 and L/150.

Durability testing comprised of two parts: 1) an investigation into the change in unit weight and compressive strength after being exposed to chemical substances for 120 days, and 2) an examination of chloride penetration resistance using the rapid chloride migration test. The first part involved the use of three chemical substances, namely sodium chloride, magnesium sulfate, and sulfuric acid, which were prepared at a concentration of 5%. For the second part, cylindrical specimens with a diameter of 100 millimeters and a height of 200 millimeters were prepared, and the rapid chloride migration test was carried out after the specimens were cast and cut into 50-millimeter height specimens.

Briefly, in the rapid chloride migration test, one side of the test cell (the cathode side) was filled with a sodium chloride solution at a

Table 4
Acceptance criteria for Self-compacting Concrete according to EFNARC.

Method	Unit	Minimum	Maximum
Slump flow by Abrams cone	mm.	650	800
T50	second	2	5
L-Box test	-	0.8	1.0

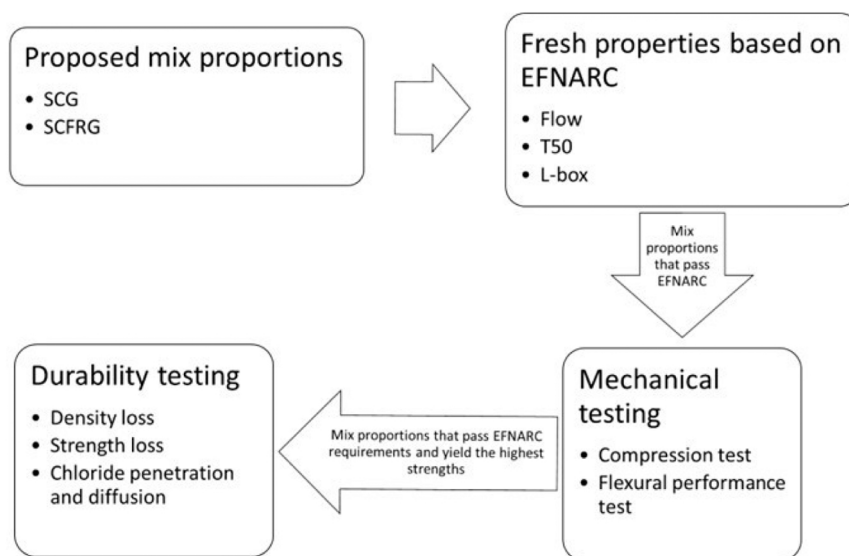


Fig. 1. Test sequence flow chart.

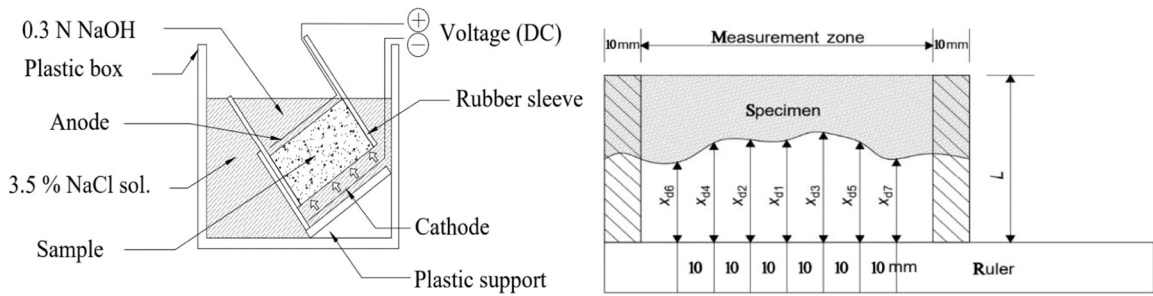


Fig. 4. Rapid chloride migration test.

a failure to meet the EFNARC limitation. In summary, the results suggest that SCG and SCFRG with an L/B ratio of 0.40 are more suitable for self-compacting geopolymer than those with an L/B ratio of 0.45.

3.1.2. T50 time

The T50 test is an essential method to evaluate the flowability of self-compacting concrete. EFNARC has set a time limit of 2–5 s for T50 in order to ensure proper flowability. A T50 value less than 2 s is not acceptable as it increases the risk of aggregate and paste segregation, while a T50 value greater than 5 s indicates inadequate flowability. In this study, the T50 test was conducted to assess the flowability of SCG and SCFRG with different L/B ratios and fiber contents.

The results of SCG and SCFRG with an L/B ratio of 0.40 are presented in Fig. 6a. The plain geopolymer demonstrated excellent flowability with a T50 of 2 s for both NaOH concentrations of 8 and 12 molars. However, the addition of steel fiber reduced the flowability and increased the T50. The highest T50 values were observed at 3.8 and 4.3 s in SCFRG with the highest fiber content (0.4/8/1.5SCFRG and 0.4/12/1.5SCFRG). The NaOH concentration level also affected flowability, with T50 increasing with increasing NaOH concentration. While SCFRG yielded higher T50 values than SCG, their values were lower than the upper limit of 5 s specified by EFNARC.

Fig. 6b shows the T50 results of SCG and SCFRG with an L/B ratio of 0.45. The increase in L/B ratio enhanced the flowability and hence reduced the T50 values. Both SCG and SCFRG demonstrated T50 values in the range of 1.0–2.3 s, indicating good flowability with or without fibers. However, the addition of fiber increased the T50, with only the SCFRG with a fiber content of 1.5% exhibiting a T50 within the acceptable range specified by EFNARC. SCG and SCFRG with fiber content less than 1% failed to meet the lower bound value of 2 s set by EFNARC.

In conclusion, the T50 test results indicate that SCG and SCFRG with an L/B ratio of 0.40 are more suitable for self-compacting geopolymer than those with an L/B ratio of 0.45. The addition of fiber reduces flowability, and the NaOH concentration level affects flowability as well.

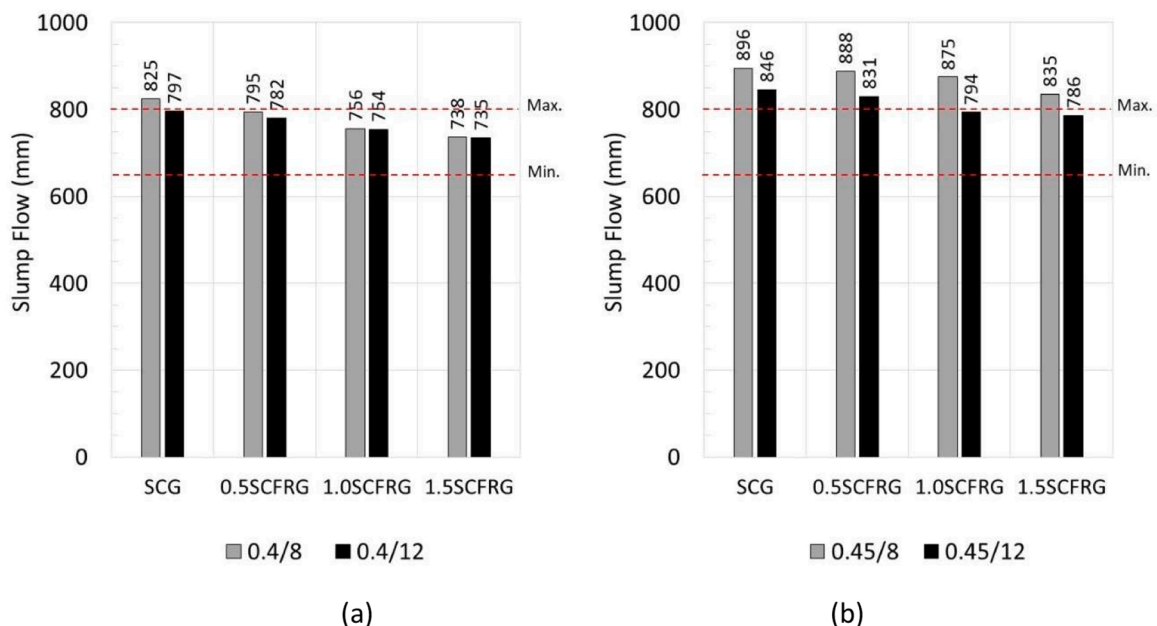


Fig. 5. Slump flow of SCG and SCFRG with L/B ratio of (a) 0.40 and (b) 0.45.

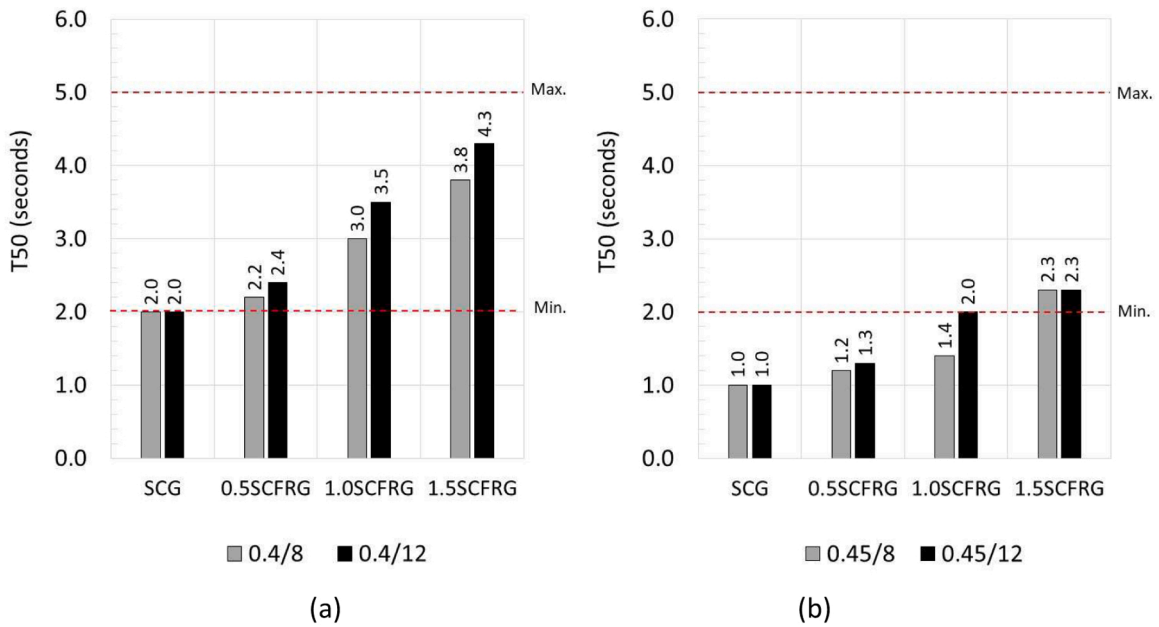


Fig. 6. T50 of SCG and SCFRG with L/B ratio of (a) 0.40 and (b) 0.45.

3.1.3. Filling ratio (L-Box)

The results of the L-Box test were analyzed to determine the passing ratio of SCG and SCFRG. Fig. 7 shows that all mixes met the EFNARC requirement for filling ability, with a passing ratio between 0.87 and 1.0. The filling ratio of SCG was generally higher than that of SCFRG by 2.5–7.7%, indicating a decrease in filling ability with the addition of fiber. An increase in liquid content, as measured by the L/B ratio, resulted in a higher filling ratio for both SCG and SCFRG, with a ratio of 0.45 providing better filling ability than a ratio of 0.40.

The effect of NaOH concentration on passing ratio was also evaluated. Results indicated that passing ratio decreased by 0.2–7.6% with increasing NaOH concentration, depending on the fiber content and L/B ratio. The decrease in passing ratio was attributed to the higher viscosity of the NaOH solution with a high concentration, resulting in a decrease in filling ability.

The performance of fresh SCG and SCFRG was evaluated based on EFNARC requirements for self-compacted concrete, and results

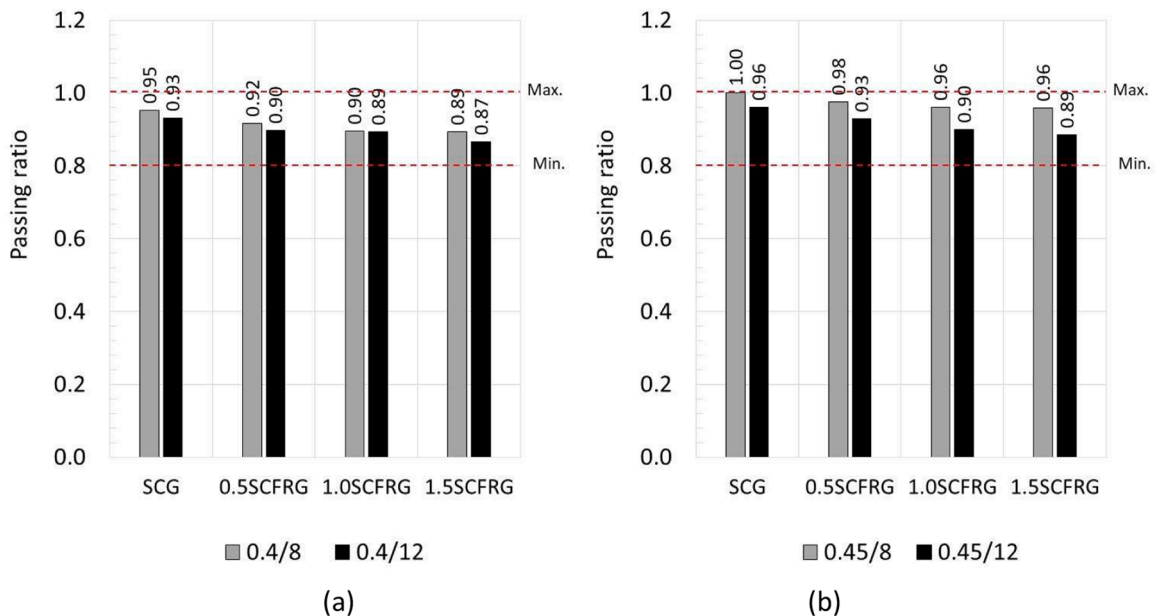


Fig. 7. Passing ratio (L-Box test) of SCG and SCFRG with L/B ratio of (a) 0.40 and (b) 0.45.

were summarized in Table 5. The filling ratio was found to be insufficiently sensitive for classifying the mixes. The T50 value was intermediate, with four mixes passing this requirement but failing the flow diameter test. The flow requirement was identified as the key factor, as the mixes that passed this requirement also passed the other two requirements (T50 and L-Box).

3.2. Mechanical properties

Based on the test results on fresh properties (Table 5), the majority of SCG and SCFRG with L/B ratio of 0.45 did not pass the EFNARC requirement and hence they were not selected. Only the mixes with L/B ratio of 0.4 with NaOH concentration of 8 and 12 molars that passed the requirements were selected for further testing on the mechanical properties.

3.2.1. Compressive strength

Fig. 8 illustrates the results for the compressive strength of SCG and SCFRG having an L/B ratio of 0.40. The compressive strength generally ranged from 58 to 64 MPa. The steel fiber volume fraction gradually increased from 0.5–1.5%, resulting in an increase in strength by approximately 3.2–8.7%. The fibers bridged the cracks and provided resistance to crack propagation, which was responsible for the increase in compressive strength. Additionally, the compressive strength increased by 0.5–3.9% as the NaOH concentration level increased from 8 to 12 molars. NaOH dissolves the glassy phase of fly ash, activating silicon and aluminum, leading to higher leaching of silica and alumina, higher geopolymerization, and better mechanical properties.

3.2.2. Flexural performance

Fig. 9 illustrates the load vs. deflection responses of SCG and SCFRG with an L/B ratio of 0.40. The load response of plain geopolymer (SCG) was brittle, as evidenced by the linear increase in load proportionate to the increase in deflection until reaching the peak load, whereupon the specimen failed abruptly, and the load dropped to zero. In contrast, fiber-reinforced geopolymer (SCFRG) demonstrated much more ductile responses. The load increased linearly with increasing deflection until the peak load, at which point cracks occurred. However, the load did not drop abruptly but gradually decreased with increasing deflection because fibers began to take over through the bridging effect across cracks and slowed the rate of crack growth.

The flexural strength was found to increase with the increase in fiber content. For fiber content ranging from 0% to 1.5% volume fractions, the flexural strengths of samples with NaOH concentrations of 8 M and 12 M increased from 2.84 to 5.95 MPa and from 3.10 to 6.54 MPa, respectively. The increase in flexural strength was mainly due to the effect of fiber bridging the cracks and enhancing the load-carrying capacity of geopolymer.

The ability of SCFRG to resist and carry load after the first crack is indicated by toughness and residual strength. Toughness is often linked to the ability of a material to absorb energy under load, and it can be determined by calculating the area under the load-deflection curve up to the deflection of L/150. While the addition of fiber at low levels does not enhance strength, it typically improves toughness. This study found that toughness increased with increasing fiber content. For plain geopolymer, the specimen ruptured as soon as the load reached its peak value, resulting in toughness values of 1.1 and 1.2 N-m for SCG with NaOH of 8 M and 12 M, respectively, up to the deflection of the peak load. SCFRG, on the other hand, exhibited significantly higher toughness than SCG. The toughness for SCFRG with NaOH of 8 M and 12 M increased by about 88% and 71%, respectively, with increasing fiber content from 0.5% to 1.5%.

Residual strength represents the remaining load-carrying capacity of the specimen after the initial cracking up to the deflection of L/150. In the case of SCG, residual strength could not be determined because there was no post-peak response. For SCFRG, residual strength ranged from 61.2% to 83.7% compared to ultimate strength, depending on fiber content and NaOH concentration level (as shown in Table 6). The residual strength increased with increasing fiber content by about 32% and 17% for SCFRG with NaOH concentrations of 8 M and 12 M, respectively.

Table 5
Fresh properties of SCG and SCFRG versus the EFNARC requirement for self-compacted concrete.

Sample type	Flow	T50	L-box
0.4/8/SCG	Not pass	Pass	Pass
0.4/8/0.5SCFRG	Pass	Pass	Pass
0.4/8/1.0SCFRG	Pass	Pass	Pass
0.4/8/1.5SCFRG	Pass	Pass	Pass
0.4/12/SCG	Pass	Pass	Pass
0.4/12/0.5SCFRG	Pass	Pass	Pass
0.4/12/1.0SCFRG	Pass	Pass	Pass
0.4/12/1.5SCFRG	Pass	Pass	Pass
0.45/8/SCG	Not Pass	Pass	Pass
0.45/8/0.5SCFRG	Not Pass	Pass	Pass
0.45/8/1.0SCFRG	Not Pass	Not Pass	Pass
0.45/8/1.5SCFRG	Not Pass	Pass	Pass
0.45/12/SCG	Not Pass	Not Pass	Pass
0.45/12/0.5SCFRG	Not Pass	Not Pass	Pass
0.45/12/1.0SCFRG	Pass	Pass	Pass
0.45/12/1.5SCFRG	Pass	Pass	Pass

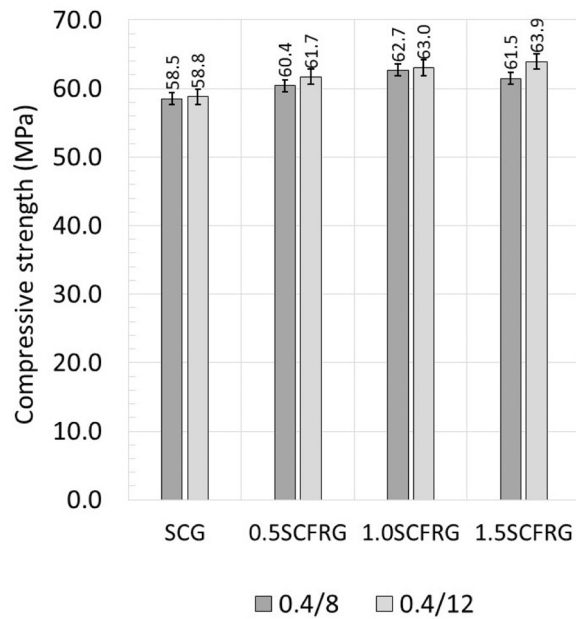


Fig. 8. Compressive strength of SCG and SCFRG with L/B ratio of 0.40.

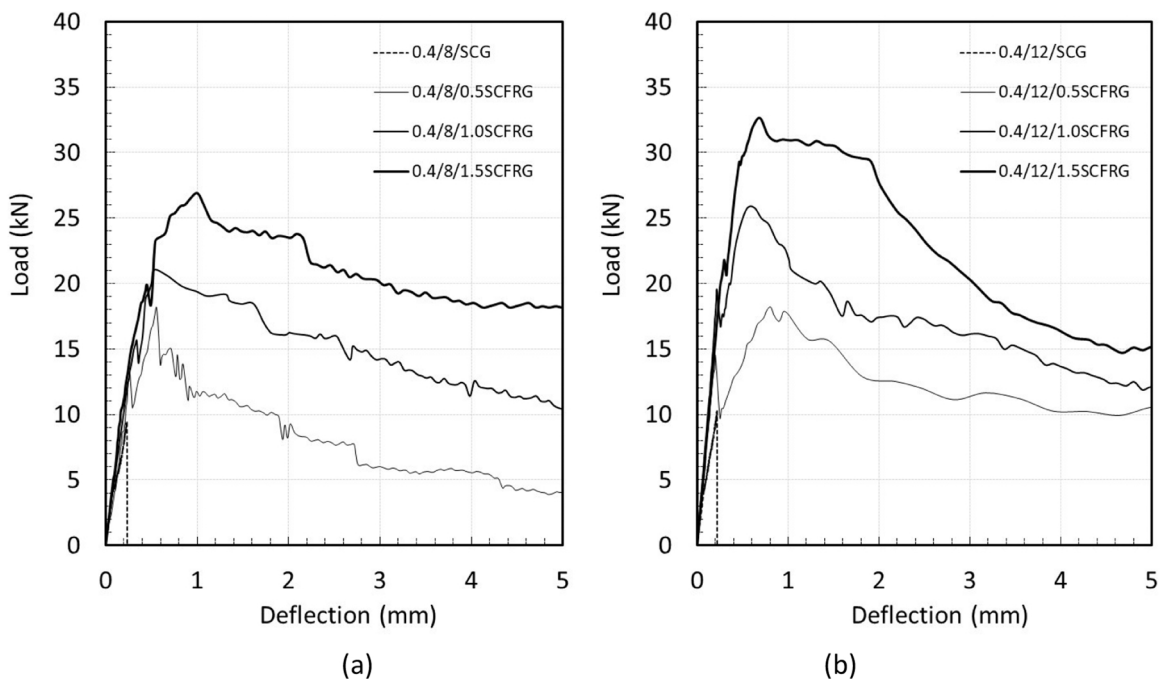


Fig. 9. Flexural response of SCG and SCFRG with L/B ratio of 0.40 and NaOH concentration of (a) 8 M and (b) 12 M.

3.3. Durability test

Based on the test results on mechanical properties, the SCFRG with 12 M NaOH had higher strength than that of 8 M NaOH. Thus, the mix with a water/binder ratio of 0.40 and 12 M NaOH, which met the EFNARC requirements for filling and flow ability and showed higher mechanical properties, was selected for durability testing. Similarly, the fiber volume fraction also varied from 0% to 1.5% in this part. All specimens were cured at room temperature for 28 days before undergoing durability tests.

Table 6
Flexural strength, toughness, and residual strength of SCG and SCFRG.

Type	First-crack strength (MPa)	Ultimate strength (MPa)	Toughness at L/150 (N-m)	Residual strength* at L/150 (%)
0.4/8/SCG	2.84	2.84	1.1	-
0.4/8/0.5SCFRG	3.93	5.44	22.2	61.2
0.4/8/1.0SCFRG	4.70	6.31	33.2	78.9
0.4/8/1.5SCFRG	5.95	8.06	41.8	80.9
0.4/12/SCG	3.10	3.10	1.2	-
0.4/12/0.5SCFRG	4.33	5.45	26.0	71.6
0.4/12/1.0SCFRG	5.86	7.74	41.1	79.6
0.4/12/1.5SCFRG	6.54	9.80	54.7	83.7

Note: *Residual strength compared to the ultimate strength

3.3.1. Weight loss

The study investigated the effect of immersion in different chemical substances on the weight of self-compacting geopolymer (SCG) and self-compacting fiber-reinforced geopolymer (SCFRG) for 120 days. The weight of the specimens was measured at the end of the immersion period in ambient conditions and in solutions of magnesium sulfate ($MgSO_4$), sulfuric acid (H_2SO_4), and sodium chloride (NaCl). The results in Fig. 10 showed that the SCFRG specimens have a higher weight than the SCG specimens in all conditions and all specimens had a reduction in weight after immersion in the chemical solutions compared to the specimens cured in ambient conditions.

Considering the impact of immersion in different solutions for 120 days on the weight of geopolymer reinforced with steel fiber, the results indicated that immersion in sodium chloride solution had no effect on the weight. One possible explanation could be the chemical composition of the geopolymer matrix. Geopolymers are known for their excellent chemical resistance, which is attributed to the formation of a dense and stable network of sodium–aluminosilicate and calcium–aluminosilicate in their gel matrix during the geopolymerization process. This network is highly cross-linked and has a low porosity, which makes it less susceptible to chemical attack and degradation. In the case of NaCl, the chloride ions may not be able to penetrate the dense geopolymer matrix and react with the aluminosilicate structure [45,46]. This may explain why the weight of the geopolymer matrix remains relatively stable even after prolonged exposure to NaCl solution.

However, immersion in $MgSO_4$ and H_2SO_4 solutions resulted in a reduction in weight of approximately 0.83–0.98% and 3.06–4.23%, respectively. A possible explanation could be because of their chemical reactions with the geopolymer material. The sulfate ions in magnesium sulfate and sulfuric acid can react with the calcium in the slag/fly ash based geopolymer, leading to the formation of calcium sulfate (gypsum) and ettringite (at low proportion), which is a less dense material. This reaction can result in the displacement of the geopolymer material and cause a reduction in weight. Additionally, the acid in sulfuric acid can also react with the alkaline geopolymer, causing it to break down and dissolve, which can further contribute to the loss in weight [46].

Comparing $MgSO_4$ and H_2SO_4 , it can be observed that the specimens submerged in $MgSO_4$ appeared to suffer more weight loss than those submerged in H_2SO_4 . Zhang et al. [47] explained that, in addition to the formation of ettringite, the dissolution of alkali causes $MgSO_4$ attack on geopolymer through the diffusion of Mg^{2+} which occurs during the migration of alkali ions into the solutions. The attack generates gypsum and brucite, decomposing the C-A-S-H phase. Gypsum is the main product in geopolymer during the attack, regardless of Na_2O concentration. Comparing SCG and SCFRG, the SCFRG exhibited weight loss within the same range of SCG. The percentage weight loss after exposure of SCG and SCFRG was about 0.83–0.98% when exposed to H_2SO_4 , and about 3.06–4.06% when exposed to $MgSO_4$.

3.3.2. Residual mechanical properties

The compressive strength of self-compacting geopolymer (SCG) and self-compacting fiber reinforced geopolymer (SCFRG) samples submerged in different chemical substances for 120 days were examined (Fig. 11). The results showed that the compressive strength of SCG samples submerged in $MgSO_4$ and H_2SO_4 decreased significantly to 62.7 MPa and 42.8 MPa, respectively, compared to the ambient sample strength of 72.1 MPa. However, the compressive strength of SCG samples submerged in NaCl remained relatively unchanged at 71.4 MPa.

On the other hand, the compressive strength of SCFRG samples submerged in $MgSO_4$, H_2SO_4 , and NaCl remained relatively stable compared to the ambient sample strength. The compressive strength of 0.5SCFRG samples submerged in H_2SO_4 was slightly reduced to 64.2 MPa, while the compressive strength of 1.0SCFRG and 1.5SCFRG samples submerged in H_2SO_4 and NaCl increased slightly to 68.1, 71.3, 78.7, and 82.5 MPa, respectively.

For self-compacting plain geopolymer (SCG), in addition to the reasons mentioned in 3.3.1, the reduction in strength when exposed to acid solutions could be attributed to the breakage of alumina-silicate bonds at high exposure to sulfuric acid. Similar findings were reported by Song et al. [49], which found a 32–37% strength reduction in geopolymer specimens exposed to 10% sulfuric acid. Bakharev [50] reported strength reduction due to zeolite formation and depolymerization of the aluminosilicate polymers in acidic media, leading to a significant loss of strength.

In the case of SCFRG, the strength loss was partly due to the deterioration of the interfacial bond between fiber and geopolymer matrix at high exposure to magnesium sulfate and sulfuric acids. Genesan [51,52] found the loss in compressive strength of both plain and fiber-reinforced geopolymer specimens to be about 20% after submersion in sulfuric acid for 180 days.

Comparing SCG and SCFRG, the strength loss of SCG was much higher than that of SCFRG. This suggests that the addition of steel

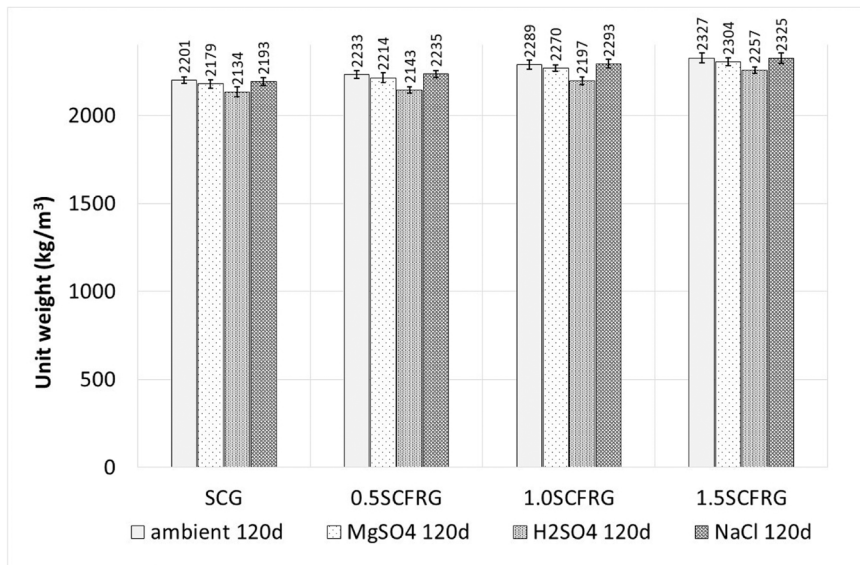


Fig. 10. Change in unit weight after 120 days of submersion in chemical substances.

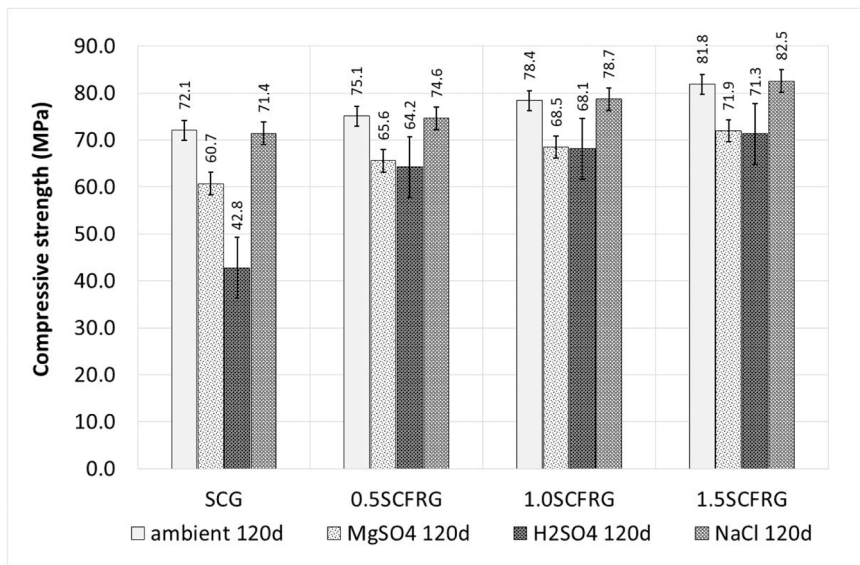


Fig. 11. Change in compressive strength after 120 days of submersion in chemical substances.

fibers in geopolymer samples can enhance durability against chemical attacks compared to plain geopolymer. There are several reasons why SCFRG samples exhibit greater stability when exposed to various chemical solutions.

Firstly, the presence of fibers can improve the mechanical properties of the geopolymer matrix, such as its tensile strength and toughness. This means that even if the geopolymer matrix experiences some loss of strength due to chemical attack, the fibers can help to maintain the overall integrity of the material by distributing stresses more evenly and preventing cracks from propagating [37,42]. Secondly, the fibers can also improve the durability of the geopolymer matrix by enhancing its resistance to cracking and deformation under different environmental conditions. This can help to minimize the amount of exposure that the geopolymer matrix has to chemical substances and reduce the overall rate of degradation and strength loss over time [52].

Overall, fiber reinforcement can be an effective strategy for improving the durability and resistance of geopolymer materials to chemical attack and can help to maintain their strength and structural integrity even in harsh environmental conditions.

3.3.3. Chloride penetration and diffusion

This part of the study investigated the chloride penetration resistance of self-compacting geopolymer (SCG) and self-compacting

fiber-reinforced geopolymer (SCFRG) by measuring the chloride penetration depth and diffusivity. The results in Table 7 indicated that the addition of steel fibers to the geopolymer matrix led to an improvement in the chloride penetration resistance.

The SCG specimen had a chloride penetration depth of 6.34 mm and a chloride diffusivity of 2.89×10^{-12} m²/s. In contrast, the SCFRG specimens had a lower chloride penetration depth and diffusivity. The 0.5SCFRG had a chloride penetration depth of 5.49 mm and a chloride diffusivity of 2.61×10^{-12} m²/s, while the 1.0SCFRG had a chloride penetration depth of 5.41 mm and a chloride diffusivity of 2.59×10^{-12} m²/s. Finally, the 1.5SCFRG had the lowest chloride penetration depth and diffusivity, with values of 4.75 mm and 2.45×10^{-12} m²/s, respectively.

The results suggest that the addition of steel fibers to the geopolymer matrix can enhance the resistance of the material to chloride ion penetration. This is attributed to the ability of steel fibers to inhibit the formation of microcracks and to bridge existing cracks, thereby reducing the permeability of the material to chloride ions. The decrease in chloride penetration depth and diffusivity with increasing fiber content indicates that a higher fiber content results in better chloride penetration resistance.

3.3.4. Visual inspection of specimen after submersion for 120 days

Visual inspection of the specimens after submersion in chemical solutions for 120 days is illustrated in Fig. 12. The following discussion provides insights based on the different types of solutions.

3.3.4.1. NaCl submersion. In the case of NaCl submersion, geopolymers typically do not react significantly with NaCl (sodium chloride) due to the inert nature of NaCl under normal conditions and the chemical composition of the geopolymer itself, which consists of aluminosilicate components formed during geopolymerization. Since NaCl is not chemically reactive with the aluminosilicate components of the geopolymer matrix, there is typically no significant chemical reaction or alteration of the geopolymer structure when geopolymer materials come into contact with NaCl. As a result, geopolymer samples submerged in NaCl tend to remain intact and undergo minimal changes [56]. This indicates the potential use of geopolymers in applications where resistance to chloride ions is desired, such as in the construction of concrete structures exposed to seawater or deicing salts.

3.3.4.2. MgSO₄ submersion. In the case of MgSO₄ submersion for 120 days, white deposits are observed all over the outer surface of the samples. Given the presence of aluminosilicate components in the geopolymer, the white crystal deposits observed on the outside surfaces of the samples submerged in the MgSO₄ solution are likely to be a combination of various crystalline compounds. One possible compound that could form is magnesium aluminum sulfate hydrate, also known as Dittmarite (MgAl₂(SO₄)₄·22 H₂O). Dittmarite is a white crystalline mineral that commonly precipitates in the presence of magnesium sulfate solutions [57,58]. Another possibility, as reported by Bakharev [59], is the diffusion of magnesium and sulfur into the surface of specimens from the exposure solution. At the same time, the migration of calcium from within the mortar matrix to the surface area occurs, leading to the formation of gypsum crystals encrusted in the geopolymer phase (CaSO₄·2H₂O). Gypsum and ettringite are known to cause expansion in cement concrete when exposed to sulfate solutions [60].

The specimens also showed signs of swelling and cracks along the outer edges. The observed swelling can be attributed to the expansion of these hydrated compounds upon crystallization or hydration. The accumulation of these crystals can exert pressure on the surrounding geopolymer matrix, leading to swelling, cracking, and potential strength loss as discussed earlier.

3.3.4.3. H₂SO₄ submersion. When geopolymer specimens are submerged in H₂SO₄ (sulfuric acid) for 120 days, they exhibit discoloration, a porous appearance, as well as signs of swelling and cracking along the edges. These observations indicate a chemical reaction and degradation of the geopolymer matrix. Sulfuric acid is a strong acid that can react with the components of the geopolymer. One possible reaction is the acid attack on the aluminosilicate components of the geopolymer matrix. Sulfuric acid can dissolve or leach out the reactive components from the geopolymer structure. This dissolution weakens the matrix and leads to the formation of pores, resulting in the observed porous appearance [61].

The discoloration, indicated by a yellow shade, can be attributed to the formation of sulfur dioxide (SO₂). This is produced through the reaction of ferric oxide (Fe₂O₃) with H₂SO₄, resulting in the dissolution of ferric oxide and the production of Fe₂(SO₄)₃ + H₂O [56].

The swelling and cracking along the edges are likely due to the formation of crystals and deposits inside the pores and air voids resulting from the leaching of sodium and calcium during the acid attack. Additionally, the reaction of calcium with sulfate anions present in the solution leads to the formation and deposition of gypsum crystals within the corroding layer [56,61]. These gypsum crystals can induce internal stresses within the geopolymer matrix, ultimately leading to expansion, cracking of the corroding layer, and a loss in strength, as discussed earlier.

Table 7
Chloride penetration depth and diffusivity.

Specimen	Penetration Depth (mm)	Chloride diffusivity ($\times 10^{-12}$ m ² /s)
SCG	6.34	2.89
0.5SCFRG	5.49	2.61
1.0SCFRG	5.41	2.59
1.5SCFRG	4.75	2.45

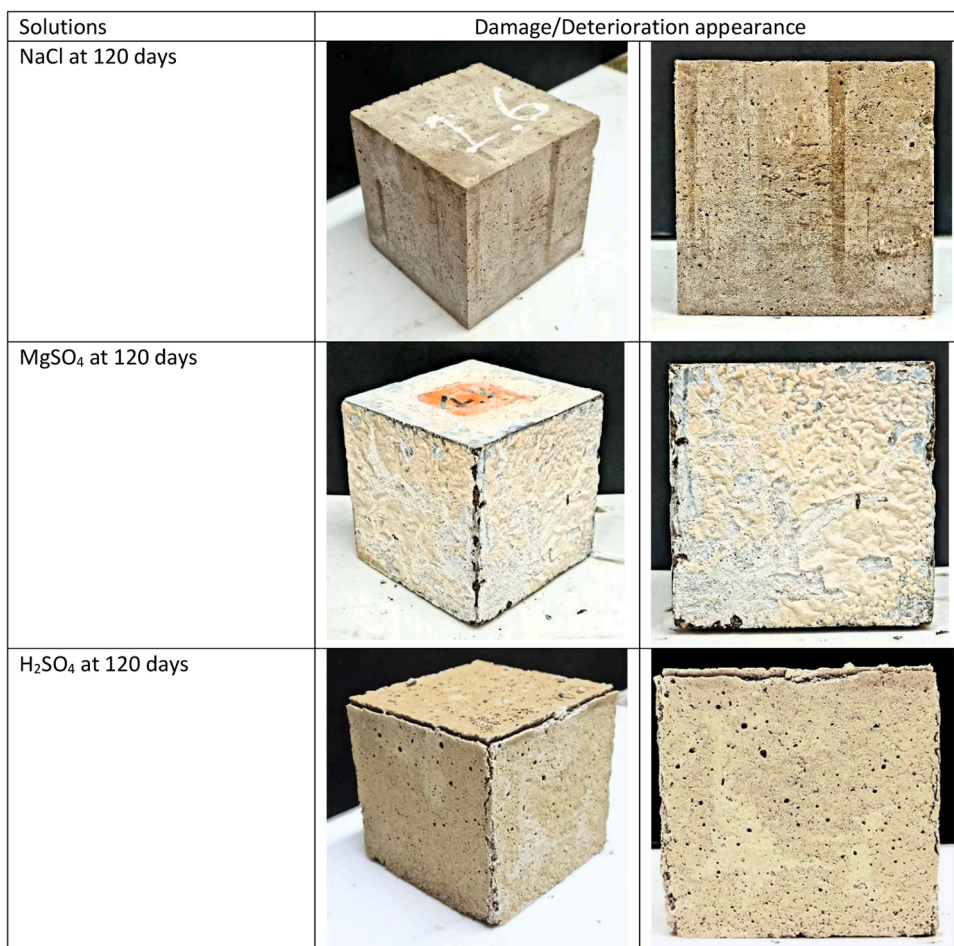


Fig. 12. Specimen appearance after submersion for 120 days.

4. Conclusion

Based on the results of these experiments, the following conclusions can be drawn:

- The EFNARC requirements of a flow of 600–800 mm, T50 of 2–5 s, and filling ratio (L-box) of 0.8–1.0 were met with mixes with an L/B ratio of 0.4, except for the 0.4/8/SCG mix. The flow requirement was the key method, as the mixes that passed this method also passed the other two requirements.
- The compressive strength of the mortar slightly increased with the increased NaOH molarity and amount of steel fiber. The maximum compressive strength of 64 MPa was observed in the 0.4/12/1.5SCFRG mix.
- The flexural strength of the mortar followed the same pattern as the compressive strength, with an increase in strength with the increased NaOH molarity and amount of steel fiber. The maximum flexural strength of 9.8 MPa was obtained with the 0.4/12/1.5SCFRG mix.
- In term of durability, the results indicate that immersion in chemical solutions for 120 days had a different impact on the weight and compressive strength of SCG and SCFRG depending on geopolymer and chemical solution types.
 - Comparing between chemical solution types, immersion in NaCl solution had no effect on both weight and compressive strength. However, immersion in MgSO₄ and H₂SO₄ solutions resulted in a weight reduction of approximately 0.83–0.98% and 3.06–4.23%, respectively, as well as a reduction in compressive strength of about 12.1–15.8% and 12.9–40.6%, respectively.
 - Comparing different types of geopolymer, it is evident that the addition of fibers can enhance the durability of the material. This improvement is demonstrated by the lower rate of strength loss observed in fiber-reinforced geopolymer (SCFRG) compared to plain geopolymer (SCG).
 - Regarding chloride migration, the addition of fiber at volumes ranging from 0.5–1.5% had a positive effect on reducing the chloride penetration depth from 6.34 to 4.75 mm and diffusivity from 2.89 to 2.45 ($\times 10^{-12}$ m²/s).
 - As for the visual inspection, when exposed to NaCl, the geopolymer remains largely unaffected. On the other hand, MgSO₄ submersion results in the formation of white crystal deposits, likely composed of compounds such as Dittmarite and gypsum,

leading to swelling, cracking, and loss in strength. The reaction of geopolymer with H_2SO_4 causes discoloration, porous appearance, swelling, and cracking, attributed to the dissolution of reactive components and the formation of sulfur dioxide and gypsum crystals.

Declaration of Competing Interest

The authors declare that they have no known competing financial interests or personal relationships that could have appeared to influence the work reported in this paper.

Data Availability

No data was used for the research described in the article.

Acknowledgement

The research was funded by the National Science, Research, and Innovation Fund (NSRF) and King Mongkut's University of Technology North Bangkok (KMUTNB) under contract no. KMUTNB-FF-66-02. The first author would like to acknowledge scholarship from the National Research Council of Thailand under the Graduate Researcher Development Program.

References

- [1] Davidovits, J. (2008). *Geopolymer Chemistry and Applications*. Geopolymer Institute, Saint-Quentic, France.
- [2] J.L. Provis, J.S.J. Van Deventer, *Geopolymers: Structures, Processing, Properties and Industrial Applications*, Woodhead Publishing, Cambridge, UK, 2009, <https://doi.org/10.1533/9781845696382.1>.
- [3] J. Davidovits. *Geopolymer Chemistry and Applications, fifth ed.*, Institut Géopolymère, Geopolymer Institute,, Saint-Quentin, France, 2020.
- [4] Anil Niş, İlhan Altundal, Compressive strength performance of alkali activated concretes under different curing conditions, *Period. Polytech. Civ. Eng.* (2021), <https://doi.org/10.3311/PPci.17016>.
- [5] R. Alzebaree, M.E. Gülşan, A. Niş, A. Mohammedameen, A. Çevik, Performance of FRP confined and unconfined geopolymer concrete exposed to sulfate attacks, *Steel Compos. Struct.* 29 (2018) 201–218, <https://doi.org/10.12989/SCS.2018.29.2.201>.
- [6] R. Alzebaree, A. Çevik, A. Mohammedameen, A. Niş, M.E. Gülşan, Mechanical performance of FRP-confined geopolymer concrete under seawater attack, *Adv. Struct. Eng.* 23 (2020) 1055–1073, <https://doi.org/10.1177/1369433219886964>.
- [7] A. Niş, M. Bilenler Altundal, Durability performance of alkali-activated concretes exposed to sulfuric acid attack, *Rev. De. la Constr. J. Constr.* 22 (1) (2023) 16–35, <https://doi.org/10.7764/rdlc.22.1.16>.
- [8] S.D. Wang, X.C. Pu, S.Y. Liu, Corrosion behavior of reinforced geopolymer concrete in simulated seawater, *Mater. Des.* 56 (2014) 889–894.
- [9] J.M. Miranda, A. Fernandez-Jimenez, J.A. Gonzalez, A. Palomo, Corrosion resistance in activated fly-ash mortars, *Cem. Concr. Res.* 35 (6) (2005) 1210–1217.
- [10] M. Aljanabi, A. Çevik, A. Niş, D. Bakbak, S. Kadhim, Residual mechanical performance of lightweight fiber-reinforced geopolymer mortar composites incorporating expanded clay after elevated temperatures, *J. Compos. Mater.* 56 (2022) 1737–1752, <https://doi.org/10.1177/00219983221088902>.
- [11] S. Kadhim, A. Çevik, A. Niş, D. Bakbak, M. Aljanabi, Mechanical behavior of fiber reinforced slag-based geopolymer mortars incorporating artificial lightweight aggregate exposed to elevated temperatures, *Constr. Build. Mater.* 315 (2021), 125766, <https://doi.org/10.1016/j.conbuildmat.2021.125766>.
- [12] D.L.Y. Kong, J.G. Sanjayan, Damage behavior of geopolymer composites exposed to elevated temperatures, *Cem. Concr. Compos.* 30 (10) (2008) 986–991.
- [13] M.E. Gülşan, R. Alzebaree, A.A. Rasheed, A. Niş, A. Kurtoglu, Development of fly ash/slag based self-compacting geopolymer concrete using nano-silica and steel fiber, *Constr. Build. Mater.* 211 (2019) 271–283, <https://doi.org/10.1016/j.conbuildmat.2019.03.228>.
- [14] A. Niş, N.A. Eren, A. Çevik, Effects of nanosilica and steel fibers on the impact resistance of slag based self-compacting alkali-activated concrete, *Ceram. Int.* 47 (17) (2021) 23905–23918, <https://doi.org/10.1016/j.ceramint.2021.05.099>.
- [15] H.Y. Zhang, V. Kodur, B. Wu, J. Yan, Z.S. Yuan, Effect of temperature on bond characteristics of geopolymer concrete, *Constr. Build. Mater.* 163 (2018) 277–285, <https://doi.org/10.1016/j.conbuildmat.2017.12.043>.
- [16] P. Chindaprasirt, P. Sukontasukkul, A. Techaphathanakon, S. Kongtun, C. Ruttanapun, D.Y. Yoo, W. Tangchirapat, S. Limkatanyu, N. Banthia, Effect of Graphene Oxide on Single Fiber Pullout Behavior, *Constr. Build. Mater.* 280 (2021), 122539, <https://doi.org/10.1016/j.conbuildmat.2021.122539>.
- [17] P. Topark-ngarm, P. Chindaprasirt, V. Sata, Setting time, strength, and bond of high-calcium fly ash geopolymer concrete (7), *J. Mater. Civ. Eng.* 27 (7) (2015) 04014198, [https://doi.org/10.1061/\(ASCE\)MT.1943-5533.0001157](https://doi.org/10.1061/(ASCE)MT.1943-5533.0001157).
- [18] P. Nuaklong, N. Boonchoo, P. Jongvivatsakul, T. Charinpanitkul, P. Sukontasukkul, Hybrid effect of carbon nanotubes and polypropylene fibers on mechanical properties and fire resistance of cement mortar, *Constr. Build. Mater.* 275 (2021), 122189, <https://doi.org/10.1016/j.conbuildmat.2020.122189>.
- [19] Piti Sukontasukkul Manote Sappakittipakorn, Prinya Chindaprasirt Hiroshi Higashiyama, Nemkumar Banthia, Properties of hooked end steel fiber reinforced acrylic modified concrete, *Constr. Build. Mater.* 186 (2018) 1247–1255, <https://doi.org/10.1016/j.conbuildmat.2018.08.055>.
- [20] P. Sukontasukkul, S. Jamnam, M. Sappakittipakorn, K. Fujikake, P. Chindaprasirt, Residual flexural behavior of fiber reinforced concrete after heating, *Mater. Struct.* 51 (2018) 98, <https://doi.org/10.1617/s11527-018-1210-3>.
- [21] P. Sukontasukkul, P. Jamsawang, Use of steel and polypropylene fibers to improve flexural performance of deep soil-cement column, *Constr. Build. Mater.* 29 (2012) 201–205, <https://doi.org/10.1016/j.conbuildmat.2011.10.040>.
- [22] P. Sukontasukkul, S. Mindess, N. Banthia, Properties of confined fibre-reinforced concrete under uniaxial compressive impact, *J. Cem. Concr. Res.* 35 (1) (2005) 11–18, <https://doi.org/10.1016/j.cemconres.2004.05.011>.
- [23] P. Sukontasukkul, S. Mindess, The shear fracture of concrete under impact loading using end confined beams, in: *Materials and Structures-Special Issue of Concrete Science and Engineering*, 36, RILEM, 2003, pp. 372–378, <https://doi.org/10.1007/BF02481062>.
- [24] F.A. Memon, M.F. Nuruddin, S. Khan, N.A. Shafiq, T. Ayub, Effect of sodium hydroxide concentration on fresh properties and compressive strength of self-compacting geopolymer concrete, *J. Eng. Sci. Technol.* 8 (2013) 44–56.
- [25] M.F. Nuruddin, S. Demie, M.F. Ahmed, N. Shafiq, Effect of superplasticizer and NaOH molarity on workability, compressive strength and microstructure properties of self-compacting geopolymer concrete, *Int. J. Geol. Environ. Eng.* 3 (2011) 187–194.
- [26] M.F. Nuruddin, S. Demie, N. Shafiq, Effect of mix composition on workability and compressive strength of self-compacting geopolymer concrete, *Can. J. Civ. Eng.* 38 (2011) 1196–1203, <https://doi.org/10.1139/A11-077>.
- [27] F.A. Memon, M.F. Nuruddin, S. Demie, Effect of superplasticizer and extra water on workability and compressive strength of self-compacting geopolymer concrete, *Res. J. Appl. Sci., Eng. Technol.* 4 (2012) 407–414.
- [28] F.A. Memon, M.F. Nuruddin, N. Shafiq, Effect of silica fume on the fresh and hardened properties of fly ash-based self-compacting geopolymer concrete, *Int. J. Min. Metall. Mater.* 20 (2013) 205–213, <https://doi.org/10.1007/s12613-013-0714-7>.

- [29] F.A. Memon, F. Nuruddin, S.U. Khan, N. Shafiq, T. Ayub, Effect of Sodium Hydroxide Concentration on Fresh Properties and Compressive Strength of Self-Compacting Geopolymer Concrete *J. Eng. Sci. Technol.*, 8, 44-56. Singh, N. B., Mishra, A. (2018). Self-Compact. geopolymer Concr.: A Rev. Constr. Build. Mater. 174 2013 274 284.
- [30] Sari A.N., Srisunarsih, E., Sucipto, T.L.A. (2021). The Use of Rice Husk Ash in Enhancing the Material Properties of Fly Ash-Based Self Compacted Geopolymer Concrete. *Journal of Physics.: Conference Series*, 1808 012011. DOI 10.1088/1742-6596/1808/1/012011.
- [31] R.K. Sandhu, R. Siddique, Influence of rice husk ash (RHA) on the properties of self-compacting concrete: A review, *Constr. Build. Mater.* 153 (2017) 751–764, <https://doi.org/10.1016/j.conbuildmat.2017.07.165>.
- [32] Sondakh, C., Gumalang, S. (2020). The processing, properties and optimum mix of fly ash based - self compacting geopolymer concrete. *IOP Conference Series: Earth and Environmental Science*. 419, 012067.
- [33] P. Yoosuk, C. Suksiripattanapong, P. Sukontasukkul, P. Chindapasirt, Properties of polypropylene fiber reinforced cellular lightweight high calcium fly ash geopolymer mortar, *Case Stud. Constr. Mater.* 15 (2021), e00730, <https://doi.org/10.1016/j.cscm.2021.e00730>.
- [34] D. Intarabut, P. Sukontasukkul, T. Phoo-Ngernkham, H. Zhang, D.-Y. Yoo, S. Limkatanyu, P. Chindapasirt, Influence of graphene oxide nanoparticles on bond-slip reponses between fiber and geopolymer mortar, *Nanomaterials* 12 (6) (2022) art. no. 943.
- [35] A. Mahmood, M.T. Noman, M. Pechočiaková, N. Amor, M. Petrù, M. Abdelkader, J. Militký, S. Sozcu, S.Z.U. Hassan, Geopolymers and fiber-reinforced concrete composites in civil engineering, *Polymers* 13 (2021) 2099, <https://doi.org/10.3390/polym13132099>.
- [36] P. Sukontasukkul, P. Chindapasirt, P. Pongsopha, T. Phoo-Ngernkham, W. Tangchirapat, N. Bantia, Effect of fly ash/silica fume ratio and curing condition on mechanical properties of fiber-reinforced geopolymer, *J. Sustain. Cem.-Based Mater.* 9 (4) (2020) 218–232, <https://doi.org/10.1080/21650373.2019.1709999>.
- [37] S. Samal, I. Blanco, An application review of fiber-reinforced geopolymer composite, *Fibers* 9 (4) (2021) 23, <https://doi.org/10.3390/fib9040023>.
- [38] S. Yan, P. He, D. Jia, Z. Yang, X. Duan, S. Wang, Y. Zhou, Effect of fiber content on the microstructure and mechanical properties of carbon fiber felt reinforced geopolymer composites, *Ceram. Int.* 42 (6) (2016) 7837–7843, <https://doi.org/10.1016/j.ceramint.2016.01.197>.
- [39] P. Behera, V. Baheti, J. Militký, S. Naem, Microstructure and mechanical properties of carbon microfiber reinforced geopolymers at elevated temperatures, *Constr. Build. Mater.* 160 (2018) 733–743, <https://doi.org/10.1016/j.conbuildmat.2017.11.109>.
- [40] K. Korniejenko, W.-T. Lin, H. Simonová, Mechanical properties of short polymer fiber-reinforced geopolymer composites, *J. Compos. Sci.* 4 (3) (2020) 128, <https://doi.org/10.3390/jcs4030128>.
- [41] P. Sukontasukkul, P. Pongsopha, P. Chindapasirt, S. Songpiriyakij, Flexural performance and toughness of hybrid steel and polypropylene fibre reinforced geopolymer, *Constr. Build. Mater.* 161 (2018) 37–44, <https://doi.org/10.1016/j.conbuildmat.2017.11.122>.
- [42] L. Li, C. Yan, N. Zhang, M.U. Farooqi, S. Xu, A.F. Deifalla, Flexural fracture parameters of polypropylene fiber reinforced geopolymer, *J. Mater. Res. Technol.* 24 (2023) 1839–1855, <https://doi.org/10.1016/j.jmrt.2023.03.035>.
- [43] M. Zuaiteer, H. El-Hassan, T. El-Maaddawy, B. El-Ariss, Flexural and shear performance of geopolymer concrete reinforced with hybrid glass fibers, *J. Build. Eng.* 72 (2023), 106580, <https://doi.org/10.1016/j.jobbe.2023.106580>.
- [44] K. Nazir, O. Canpolat, M. Uysal, A. Niş, O.F. Kuranlı, Engineering properties of different fiber-reinforced metakaolin-red mud based geopolymer mortars, *Constr. Build. Mater.* 385 (2023), 131496, <https://doi.org/10.1016/j.conbuildmat.2023.131496>.
- [45] EFNARC, Specification and Guidelines for Self-Compacting Concrete, 2002, Hampshire, UK.
- [46] M. Wasim, T.D. Ngo, D. Law, A state-of-the-art review on the durability of geopolymer concrete for sustainable structures and infrastructure, *Constr. Build. Mater.* 291 (2021), 123381, <https://doi.org/10.1016/j.conbuildmat.2021.123381>.
- [47] C. Gunasekara, D. Law, S. Bhuiyan, S. Setunge, L. Ward, Chloride induced corrosion in different fly ash based geopolymer concretes, *Constr. Build. Mater.* 10 (200) (2019) 502–513, <https://doi.org/10.1016/j.conbuildmat.2018.12.168>.
- [48] J. Zhang, C. Shi, Z. Zhang, X. Hu, Reaction mechanism of sulfate attack on alkali-activated slag/fly ash cements, *Constr. Build. Mater.* 318 (2022), 126052, <https://doi.org/10.1016/j.conbuildmat.2021.126052>.
- [49] M.G. Sá Ribeiro, M.G. Sá Ribeiro, P.F. Keane, M.R. Sardela, W.M. Kriven, R.A. Sá Ribeiro, Acid resistance of metakaolin-based bamboo fiber geopolymer composites, *Constr. Build. Mater.* 302 (2021), 124194, <https://doi.org/10.1016/j.conbuildmat.2021.124194>.
- [50] X.J. Song, X.J., Marosszeky, M., Brungs, M., Munn, R. (2005). Durability of Fly Ash-Based Geopolymer Concrete Against Sulphuric Acid Attack, in: International Conference on Durability of Building Materials and Components, Lyon, France.
- [51] T. Bakharev, Resistance of geopolymer materials to acid attack, *Cem. Concr. Res.* 35 (4) (2005) 658–670, <https://doi.org/10.1016/j.cemconres.2004.06.005>.
- [52] N. Ganesan, R. Abraham, D. Raj, Durability characteristics of steel fibre reinforced geopolymer concrete, *Constr. Build. Mater.* 93 (2015) 471–476, <https://doi.org/10.1016/j.conbuildmat.2015.06.014>.
- [53] X. Guo, G. Xiong, Resistance of fiber-reinforced fly ash-steel slag based geopolymer mortar to sulfate attack and drying-wetting cycles, *Constr. Build. Mater.* 269 (2021), 121326, <https://doi.org/10.1016/j.conbuildmat.2020.121326>.
- [54] N.A. Eren, R. Alzebaree, A. Çevik, A. Niş, A. Mohammedameen, M.E. Gülşan, Fresh and hardened state performance of self-compacting slag based alkali activated concrete using nanosilica and steel fiber, *J. Compos. Mater.* 55 (2021) 4125–4139, <https://doi.org/10.1177/002199832110323>.
- [55] N.A. Eren, R. Alzebaree, A. Çevik, A. Niş, A. Mohammedameen, M.E. Gülşan, The effects of recycled tire rubbers and steel fibers on the performance of self-compacting alkali activated concrete, *Period. Polytech. -Civ. Eng.* 65 (3) (2021), <https://doi.org/10.3311/PPci.17601>.
- [56] M. Albitar, M.S. Mohamed Ali, P. Visintin, M. Drechsler, “Durability evaluation of geopolymer and conventional concretes,” *Constr. Build. Mater.* vol. 136 (2017) 374–385, <https://doi.org/10.1016/j.conbuildmat.2017.01.056>.
- [57] A.K. Sarkar, Hydration/dehydration characteristics of struvite and dittmarite pertaining to magnesium ammonium phosphate cement systems, *J. Mater. Sci.* 26 (1991) 2514–2518, <https://doi.org/10.1007/BF01130204>.
- [58] Li, Z., Ding, Z., & Zhang, Y. (2004, May). Development of sustainable cementitious materials. In Proceedings of international workshop on sustainable development and concrete technology, Beijing, China (pp. 55–76).
- [59] T. Bakharev, Durability of geopolymer materials in sodium and magnesium sulfate solutions, *Cem. Concr. Res.* 35 (6) (2005) 1233–1246, <https://doi.org/10.1016/J.CEMCONRES.2004.09.002>.
- [60] C. Cau-dit-Coumes, Alternative binders to ordinary Portland cement for radwaste solidification and stabilization, *Cem.-Based Mater. Nucl. Waste Storage* (2012) 171–191, https://doi.org/10.1007/978-1-4614-3445-0_16.
- [61] A. Allahverdi, F. Skvara, Sulfuric acid attack on hardened paste of geopolymer cements-Part 1. Mechanism of corrosion at relatively high concentrations, *Ceram. Silik.* 49 (4) (2005) 225.